Journal of Alloys and Compounds 489 (2010) 570–575

Contents lists available at ScienceDirect

Journal of Alloys and Compounds

journal homepage: www.elsevier.com/locate/jallcom

The effect of rare earth elements on the kinetics of the isothermal coarsening of the globular solid phase in semisolid AZ91 alloy produced via SIMA process

B. Nami [a], S.G. Shabestari [a,*], S.M. Miresmaeili [b], H. Razavi [a], Sh. Mirdamadi [a]

[a] Department of Materials and Metallurgical Engineering, Iran University of Science and Technology (IUST), Narmak, Tehran, Iran
[b] Department of Mechanical Engineering, Shahid Radjaei University, Lavizan, Tehran, Iran

ARTICLE INFO

Article history:
Received 14 January 2009
Received in revised form
21 September 2009
Accepted 22 September 2009
Available online 25 September 2009

Keywords:
Magnesium
Rare earth elements
Semisolid
Kinetics
Microstructure

ABSTRACT

In the present study, the effects of rare earth (RE) elements on the microstructure and coarsening kinetics of the solid globular particle in the semisolid slurry of AZ91 magnesium alloy have been studied at 570 °C and 580 °C. The results showed that the coarsening kinetics of the solid globular particles in semisolid slurry of AZ91 alloy satisfies the Ostwald ripening theory. It was shown that the coarsening rate of the solid particles decreases by adding RE elements into AZ91 alloy, specially at 580 °C, which results in the smaller particles size. It was attributed to the solid–liquid interfacial energy reduction due to the addition of RE elements.

1. Introduction

Magnesium alloys are being increasingly used in the automotive industry in order to reduce the weight of the cars, thereby reducing fuel consumption and environmental pollution. AZ91 alloy is the most favorite magnesium alloy, being used in the approximately 90% of all the magnesium cast products [1]. However, its applications are limited to certain parts of the vehicles because of its poor creep strength and mechanical properties at high temperatures [1–4].

It has been shown that the ambient and high temperature mechanical properties of AZ91 alloy can be improved by the small addition of RE elements [2]. On the other hand, the casting defects, such as hot tearing, limit the addition of these elements into magnesium alloys and consequently restrict the development of RE containing magnesium alloys [5].

Semisolid metal (SSM) processing is a new technology for near net-shape production of engineering components, in which alloys are processed at a temperature between solidus and liquidus temperatures [6]. The advantages of SSM process compared with conventional die casting process are lower operating temperatures, laminar flow during mold filling and reduced solidification shrinkage. Consequently, one may expect longer die life, shorter cycle time, reduced gas entrapment and porosity, and particularly lower tendency to hot tearing [6].

The effect of RE elements on the microstructure of magnesium alloys has previously been studied [2]. In the present study, the effects of these elements on the microstructure and isothermal coarsening kinetics of the globular α(Mg) phase were investigated in a semisolid AZ91 magnesium alloy produced via strain induced melt activation (SIMA) process.

2. Experimental

Two alloys AZ91 (Mg–8 at.% Al–0.32 at.% Zn–0.11 at.% Mn) and AZR911 (Mg–8.2 at.% Al–0.32 at.% Zn–0.1 at.% Mn–0.17 at.% RE as lanthanum base misch metal) were used. The test specimens were melted in a cylindrical mild steel cup with 38 mm diameter, 100 mm height and 0.2 mm wall thickness in a vertical tube furnace under the protection of air + SO_2 gas mixture at 630 ± 2 °C for 25 min. Subsequently, the steel cup containing the melt was quenched into water at room temperature. The castings were then machined to a round shape with the dimension of 30 mm diameter and 10 mm height and were compressed about 10% at 250 °C using a hydraulic pressure machine and subsequently quenched in cold water. The compressed specimens were isothermally heated at 570 ± 2 °C and 580 ± 2 °C for different periods of time between 0 min and 120 min before quenching into cold water. To ensure the conditions of isothermal holding during semisolid treatment, the samples water quenching were carried out after heating for 50 min. Therefore, the beginning time of isothermal holding was defined as the time when the samples were heated for 50 min.

Samples for thermal analysis were melted in a graphite crucible in an electrical resistance furnace at 670 °C for 30 min, and then a K-type thermocouple was placed at the center of the crucible that was insulated from the top and the bottom. The crucible together with the thermocouple was removed from the furnace and allowed to be cooled in air. The temperature changes were continuously recorded during

* Corresponding author.
E-mail address: shabestari@iust.ac.ir (S.G. Shabestari).

0925-8388/$ – see front matter © 2009 Elsevier B.V. All rights reserved.
doi:10.1016/j.jallcom.2009.09.112

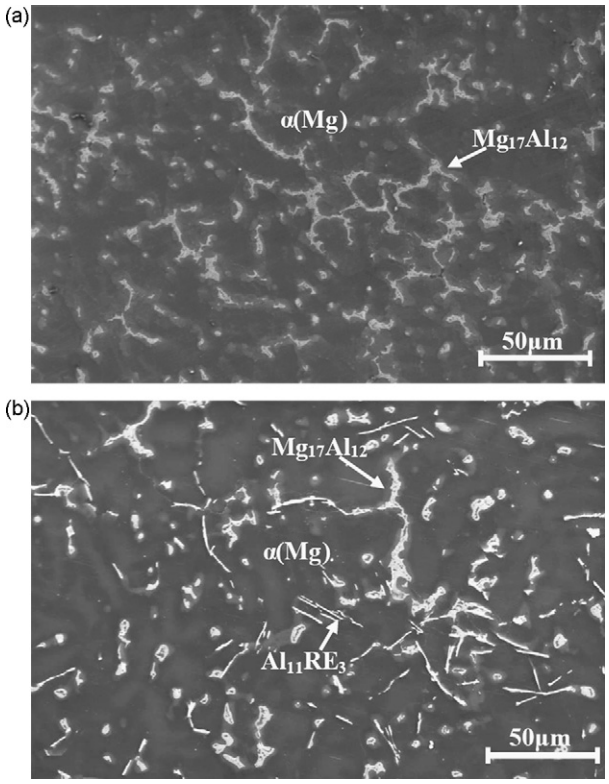

Fig. 1. As cast microstructure of (a) AZ91 alloy and (b) AZR911 alloy.

the solidification process using a high-speed data acquisition system linked to a computer.

Samples for metallographic investigations were prepared, polished, and etched with 1% nital solution (1 cm^3 HNO_3 and 99 cm^3 ethylic alcohol). The microstructure of the samples was studied and analyzed using a scanning electron microscope (SEM) equipped with energy dispersive X-ray spectroscopy (EDX). X-ray diffraction (XRD) was used in order to investigate and identify the existing phases in the specimens.

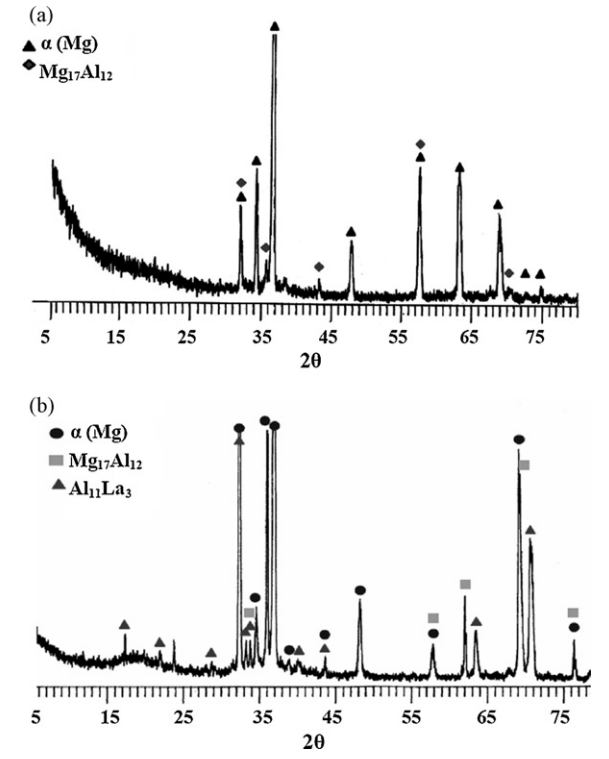

Fig. 2. XRD patterns of (a) as cast AZ91 alloy and (b) as cast AZR911 alloy.

Table 1
Chemical composition (at.%) of the indicated phases in Fig. 1b.

	Mg	Al	Zn	La	Ce
α(Mg)	97.24	2.76	–	–	–
$Mg_{17}Al_{12}$	60.97	32.67	6.36	–	–
$Al_{11}RE_3$	13.58	64.62	0.8	17.8	3.2

Quantitative metallography of the specimens was carried out using Clemex vision image analysis software. At least five representative areas with the total surface of 30 mm^2 in each sample were studied through metallographic evaluations. The shape factor (*SF*) is defined as $SF = 4\pi A/P^2$ where *A* and *P* are the area and the perimeter of the primary particles, respectively.

The circular diameter of the primary α(Mg) particles (*D*) was calculated based on the diameter of a circle having the same area as the measured object, using the following equation [7]:

$$D = 2\sqrt{\frac{A}{\pi}} \quad (1)$$

3. Results and discussions

The SEM images of AZ91 and AZR911 alloys are shown in Fig. 1. As shown, the microstructure of AZ91 alloy is composed of α(Mg) and β($Mg_{17}Al_{12}$) phases which have been verified by XRD pattern in Fig. 2a. As seen, the β($Mg_{17}Al_{12}$) phase has been mainly distributed at the interdendritic regions. It is observed that the amount of β($Mg_{17}Al_{12}$) phase has significantly decreased and new needle-shaped intermetallic phase has been formed in the microstructure of AZR911 alloy (Fig. 1b). Based on the XRD pattern of AZR911 alloy (Fig. 2b), the new phase is $Al_{11}RE_3$ intermetallic.

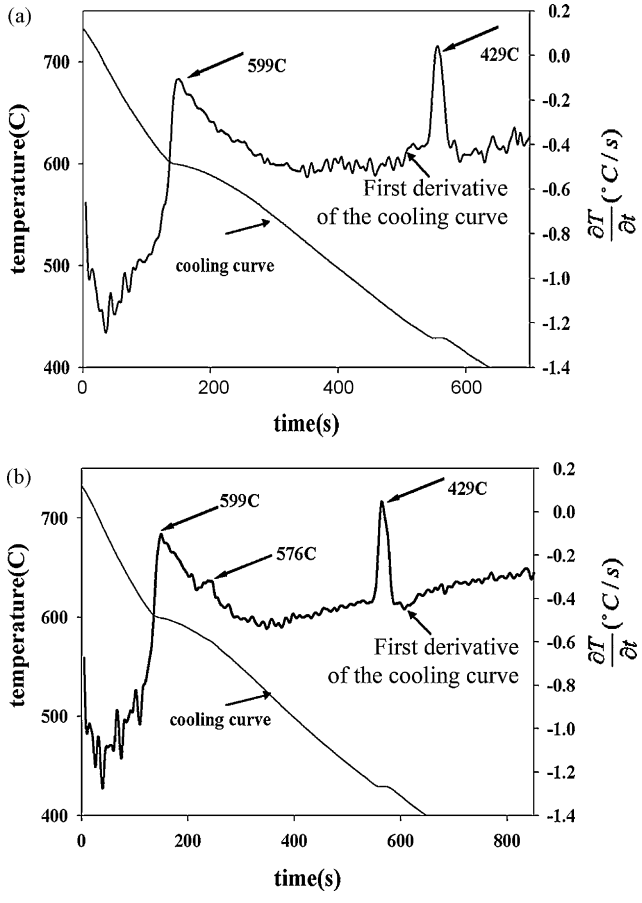

Fig. 3. Cooling curve of the alloys solidification with their first derivative curve (a) AZ91 alloy and (b) AZR911 alloy.

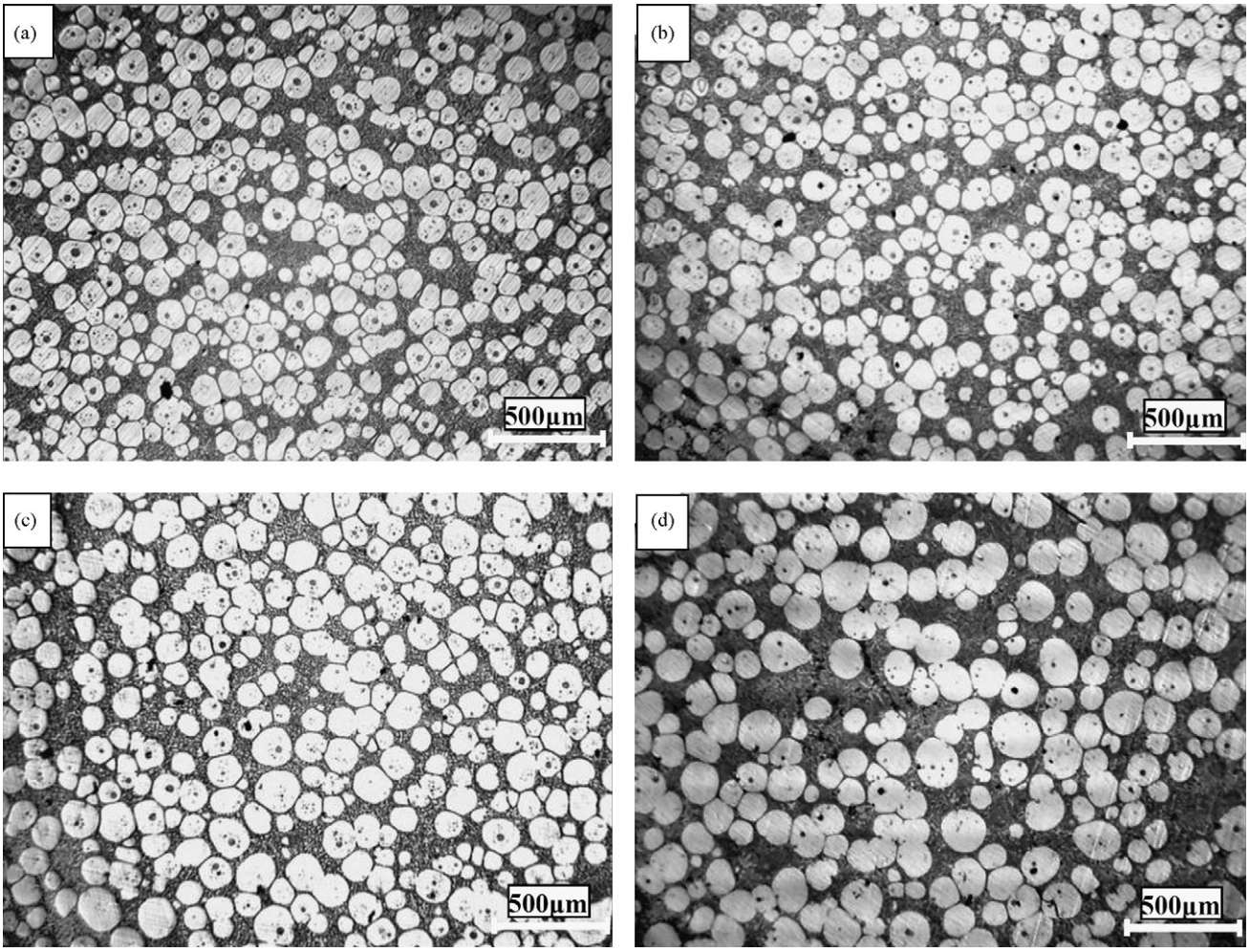

Fig. 4. Semisolid microstructure of AZ91 alloy at 580 °C for (a) 0 s, (b) 900 s, (c) 3600 s, and (d) 7200 s.

The chemical composition of the indicated phases in Fig. 1b is presented in Table 1. As shown, the solubility of RE elements in the α(Mg) and $Mg_{17}Al_{12}$ phases is negligible and they have been concentrated in the acicular $Al_{11}RE_3$ intermetallic phase.

The cooling curves of AZ91 and AZR911 alloys are shown in Fig. 3. The first derivative of the cooling curve (dT/dt) was calculated to enhance the slope changes that are related to the solidification reaction for the different phases, and to facilitate the determination of the critical solidification characteristics of the alloys.

Two peaks are observed in the derivative of the cooling curve of AZ91 alloy at 599 °C and 429 °C, which correspond to the formation of primary α(Mg) phase and non-equilibrium eutectic reaction $L \rightarrow \alpha(Mg) + Mg_{17}Al_{12}$, respectively. As shown in Fig. 3b, the addition of rare earth elements to AZ91 alloy has no considerable influence on the start and finish temperatures of the alloy solidification. However a new peak appears at 576 °C and it is confirmed that this peak can be attributed to the formation of RE containing intermetallic according to the reaction $L \rightarrow L + \alpha(Mg) + AL_{17}RE_{12}$ [8]. Therefore, the lowered amount of β($Mg_{17}Al_{12}$) intermetallic phase in AZR911 alloy is resulted from the consumption of Al atoms due to the formation of $Al_{11}RE_3$ intermetallic at the initial stages of the alloy solidification.

Fig. 4 shows the semisolid microstructure of AZ91 alloy which has isothermally been treated at 580 °C for different periods of holding time. As seen, the microstructure in the semisolid state consists of fine and spherical primary α(Mg) particles which are uniformly distributed in a matrix. The matrix has been formed during the subsequent solidification of the remained liquid in the semisolid slurry during quenching into water. It is observed that the size of particles is increased with the holding time.

Fig. 5 shows the microstructures produced through the solidification of remained liquid in AZ91 and AZR911 alloys which have been quenched from 570 °C. The solidification of the remaining liquid produces further α(Mg) particles which indicated by B (the dark area). It is followed by the formation of a continuous eutectic network of $Mg_{17}Al_{12}$ intermetallic (the gray area). As shown, the fine particles have been formed in the last solidified region of the semisolid AZ91 and AZR911 samples. The EDX analyses of these particles are presented in Table 2. It indicates that they are Al_8Mn_5 and $Al_{11}RE_3$ intermetallics in AZ91 and AZR911 alloys, respectively. It can be observed that the morphology of $Al_{11}RE_3$ intermetallic has changed to quadrangle shape after semisolid treatment.

Fig. 6 shows the variations of the particle size, the particle density, the solid fraction, and the shape factor with the holding time in the semisolid slurry of AZ91 and AZR911 alloy at 570 °C and 580 °C. It can be observed that the size of the particles in both alloys increases with the holding time, while the particle density

Table 2
Chemical composition (at.%) of the indicated phases in Fig. 5.

Phase	Mg	Al	Zn	La	Ce	Pr	Mn
A	4.29	57.59	–	–	–	–	36.90
C	10.10	69.71	0.49	15.94	2.04	1.73	–

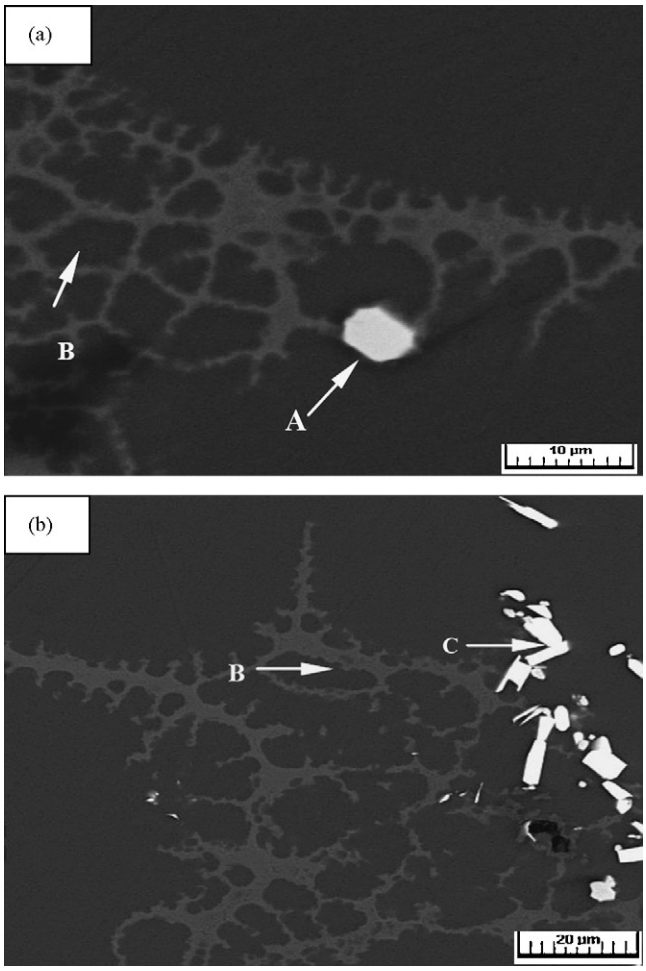

Fig. 5. SEM microstructure of (a) AZ91 alloy and (b) AZR911 alloy in the semisolid state treated at 570 °C for 3600 s.

decreases with the holding time. As shown, the volume fraction of the solid phase increases by decreasing the holding temperature from 580 °C to 570 °C. As shown in Fig. 6a, the particle size has decreased due to the addition of RE elements into AZ91 alloy at all the holding time. However, it is evident that the holding time and rare earth elements have no significant effect on the volume fraction and the shape factor of α(Mg) phase in the both alloys.

Therefore, the investigation of the particles coarsening with holding time is necessary for understanding the changes that resulted due to the addition of RE elements.

There is a reasonable agreement in the literatures showing that the main mechanism of grain coarsening in semisolid slurries is Ostwald ripening in which the grain growth takes place in the liquid matrix [9–12]. The driving force for grain coarsening by Ostwald ripening is the reduction of interfacial free energy when large grains grow and small ones shrink. According to Ostwald ripening mechanism, the rate of grain coarsening is controlled by a diffusional mechanism as the following equation [13,14]:

$$\bar{D}^3 - \bar{D}_0^3 = kt \tag{2}$$

where $\bar{D}$ is the average diameter of grains, $\bar{D}_0$ is the initial average diameter of grains, t (s) is the holding time, and k is the coarsening rate and obtained using the following equation [12]:

$$k = \frac{64}{9}\frac{\Gamma D_l T}{m_l(C_S - C_l)}F(V_V) \tag{3}$$

where T is the coarsening temperature, m_l is the slope of the liquidus curve, C_s and C_l are the concentration of the solute atom in the solid and liquid phases at the coarsening temperature, $F(V_V)$ is a function of the solid phase volume fraction, D_l is the liquid interdiffusion coefficient, and Γ is the capillary length which defined as [12]:

$$\Gamma = \frac{V^s\gamma}{\Delta H^S} \tag{4}$$

where γ is the solid–liquid interfacial energy, V^S is the molar volume of the solid, and ΔH^S is the enthalpy of fusion.

Table 3 presents the relevant parameters for AZ91 alloy at 580 °C which introduced in Eq. (3) yields the theoretical value of the coarsening rate equal to 237 $\mu m^3\,t^{-1}$.

The metallographic observation of the specimens showed that the volume fraction of the solid α(Mg) particles decreases with the holding time up to about 50 min and after that it remains constant. It was also observed that the globularization of the primary dendrites had not been completed up to about 50 min. Therefore the beginning time of isothermal holding was defined as the time when the samples were heated for 50 min.

The experimental values of k were calculated by the least-square fit of kinetics equation (Eq. (2)) to the average diameter of α(Mg) particles obtained from quantitative analysis in a plot of $\bar{D}^3 - \bar{D}_0^3$ versus t as shown in Fig. 7.

The theoretical value of the coarsening rate of solid particles in semisolid slurry of AZ91 alloy at 580 °C (237 $\mu m^3\,t^{-1}$) shows a very good agreement with its experimentally calculated value (227 $\mu m^3\,t^{-1}$) at the same temperature.

The linear relationship between $\bar{D}^3 - \bar{D}_0^3$ and the holding time and the experimentally obtained coarsening rate suggests that the classical Ostwald ripening theory can be applied for coarsening of the solid particles in semisolid slurries of AZ91 alloy.

As shown in Fig. 6, rare earth elements addition results in smaller particle size and the higher particle density in comparison with AZ91 alloy at two temperatures. Correspondingly, it is clearly seen in Fig. 7 that the coarsening rate of the solid particles has been decreased in AZR911 alloy. In other words, the growth of primary α(Mg) particles has been restricted by adding RE elements.

To understand this phenomenon, Eqs. (3) and (4) can be referred. According to the equations, it can be concluded that two physical parameters of diffusion coefficient and solid–liquid interfacial energy play main role in determining the coarsening rate. It has been proved that rare earth elements are surface-active elements and they can decrease the surface energy of the alloys melt [20,21]. Therefore, the decreasing of coarsening rate for AZR911 alloy at 580 °C is attributed to the reducing of the solid–liquid interfacial energy due to the addition of RE elements. However, Fig. 7 shows that rare earth elements have no considerable effect on the coarsening rate of AZ91 alloy at 570 °C. The different effect of RE on the coarsening rate can be explained using the cooling curve of AZR911 alloy. As shown in Fig. 3, the forming temperature of $Al_{11}RE_3$ intermetallic is about 576 °C. In such a case, it is expected that at the temperatures below 576 °C the concentration of RE elements in the remained liquid is depleted due to the formation of $Al_{11}RE_3$ intermetallic. Therefore, there seems to be no considerable amount of

Table 3
Parameters of the modified Ostwald ripening equation for AZ91 alloy at 580 °C.

C_l (at.%Al)	C_s (at.%Al)	m_l (K/at.%Al)	γ (Jm^{-2})	D_l ($m^2\,s^{-1}$)	ΔH^s ($J\,mol^{-1}$)	V_m ($m^3\,mol^{-1}$)	$F(V_V)$
10.8 [15]	2.6 [15]	6.87 [15]	0.09 [16]	4×10^{-9} [16]	8891 [17]	13.99×10^{-6} [18]	3.94 [19]

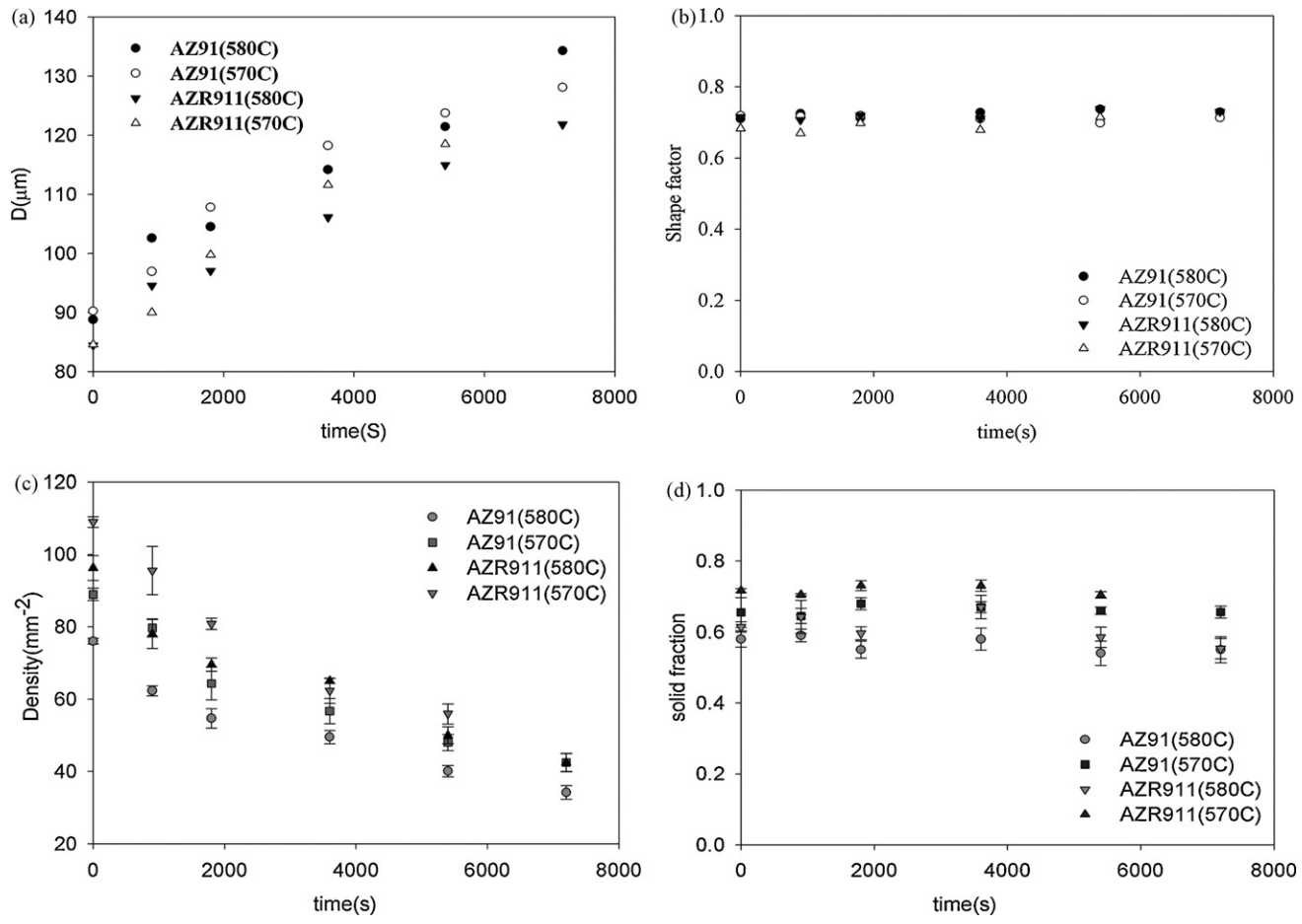

Fig. 6. Effects of isothermal holding time on the (a) particle diameter, (b) shape factor, (c) particle density, and (d) solid fraction.

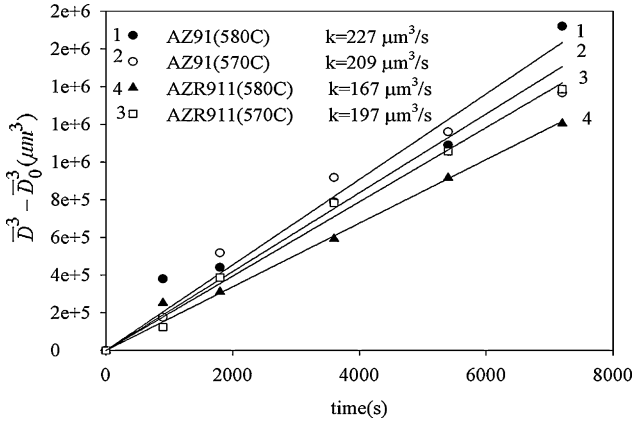

Fig. 7. Variations of $\bar{D}^3 - \bar{D}_0^3$ as a function of isothermal holding time.

rare earth elements in the remained liquid to affect the solid–liquid interfacial energy at 570 °C. In other word, the solid–liquid interfacial energy of AZR911 alloy at 580 °C is less than that its value at 570 °C.

4. Conclusions

The effects of rare earth (RE) elements on the microstructure and coarsening kinetics of the solid globular particle in the semisolid slurry of AZ91 magnesium alloy have been studied at 570 °C and 580 °C. The following results were obtained:

1. The as cast and semisolid microstructure of AZ91 magnesium alloy is mainly composed of α(Mg) and $Mg_{17}Al_{12}$ phases. By rare earth elements addition to AZ91 alloy, the amount of β($Mg_{17}Al_{12}$) phase decreases and a new $Al_{11}RE_3$ phase forms in the as cast and semisolid microstructure.
2. The theoretical and experimental values of coarsening rate suggest that Ostwald ripening theory can be used to describe the coarsening of the solid α(Mg) particle in the semisolid slurry of AZ91 alloy.
3. The coarsening rate of the solid particles decreases by adding RE elements into AZ91 alloy, specially at 580 °C, which results in the smaller particles size. It was attributed to the solid–liquid interfacial energy reduction caused by the addition of RE elements.

References

[1] Y. Guangyin, S. Yangshan, D. Wenjiang, Scripta Mater. 43 (2000) 1009–1013.
[2] F. Khomamizadeh, B. Nami, S. Khoshkhooei, Met. Mater. Trans. A 36 (2005) 3489–3494.
[3] G. Wu, Y. Fan, H. Gao, C. Zhai, Y.P. Zhu, Mater. Sci. Eng. A 408 (2005) 255–263.
[4] W. Qudong, C. Wenzhou, Z. Xiaoqin, L. Yizhen, J. Mater. Sci. 36 (2001) 3035–3040.
[5] Z. Weichao, L. Shuangshou, T. Bin, Z. Daben, J. Rare Earths 24 (2006) 346–351.
[6] S. Ji, Z. Fan, M.J. Bevis, Mater. Sci. Eng. A 299 (2001) 210–217.
[7] S. Nafisi, R. Ghomashchi, Mater. Sci. Eng. A 452–453 (2007) 437–444.
[8] L.Y. Wei, G.L. Dunlop, J. Alloys Compd. 232 (1996) 264.
[9] M. Ferrante, E. Freitas, Mater. Sci. Eng. A 271 (1999) 172–180.
[10] E. Manson, I. Stone, J. Jones, P. Grant, B. Cantor, Acta Mater. 50 (2002) 2517–2535.
[11] P. Voorhees, Met. Trans. 21A (1990) 27–37.
[12] S. Hardy, P. Voorhees, Met. Trans. 19A (1988) 2713–2721.
[13] I.M. Lifshitz, V.V. Slyozov, J. Phys. Chem. Solids 19 (1961) 35–38.

[14] C. Wagner, Z. Electrochem. 65 (1961) 581–586.
[15] H. Baker, Alloys Phase Diagram, ASM International, 1992.
[16] M. Li, T. Tamura, K. Miwa, Acta Mater. 55 (2007) 4635–4643.
[17] E.A. Brandes, G.B. Brook, Smithells Metals Reference Book, seventh ed., Butherworth–Heinemann, Oxford, 1992.
[18] B. Hallstedt, Calphad 31 (2007) 292–302.
[19] P.W. Voorhees, M.E. Glicksman, Met. Mater. Trans. 15A (1984) 1081–1088.
[20] Z. Xia, Z. Chen, Y. Shi, N. Mu, N. Sun, J. Electron. Mater. 31 (2002) 564–567.
[21] M. Kobashi, T. Choh, J. Mater. Sci. 28 (1993) 684–690.